URSI GASS 2020, Rome, Italy, 29 August - 5 September 2020

Clutter Loss Measurements and Modeling at 26 GHz Band

J. Huang, O. Zahid, and S. Salous*
Department of Engineering, Durham University, Durham, DH1 3LE U.K, *sana.salous@durham.ac.uk

Abstract

Clutter loss refers to the power loss caused by clutter objects such as buildings and vegetation. The determination of clutter loss is crucial for the deployment of wireless communication networks. In this paper, we present results of clutter loss measurements at 26 GHz in a campus environment. The ITU-R P.2108-0 statistical clutter loss model is applied to model the clutter loss and the cumulative distribution functions (CDFs) of the measured and modeled clutter losses are compared, which show good agreement.

1 Introduction

As defined in ITU-R P.2108-0 [1], clutter refers to objects such as buildings and vegetation, which are on the surface of the earth but not terrain. Clutter loss is defined as the difference in the transmission loss or basic transmission loss with and without the presence of terminal clutter at either end of the path with all other path details being the same.

The determination of clutter loss is crucial for the deployment of wireless communication networks, which needs to be obtained from real clutter loss measurements. Clutter loss measurements require one end of the link to be above clutter level while the other terminal is in the clutter. An illustration of clutter loss measurement setup is shown in Fig. 1. At the transmitter (Tx) side, a horn antenna is usually placed above the clutter for example on the rooftop of a building and down tilted, while the receiver (Rx) is behind clutter and equipped with an omni-directional antenna.

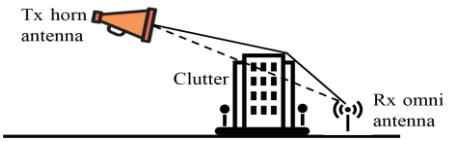

Figure 1. An illustration of clutter loss measurements.

Only a few clutter loss measurements have been reported in the literature below sub-6 GHz band, and in the millimeter wave (mmWave) band. In [2], clutter loss measurements were conducted in three cities in the US in the 1755-1780 MHz band. The median clutter loss was found to be 20-27 dB. In [3], the independent and joint clutter loss and building entry loss were measured at 3.5 GHz. The results showed that the clutter loss and building entry loss cannot be treated as multiplicative, and the combined loss was related to the details of building geometry and surrounding environment. In [4], clutter loss measurements were conducted at two bands around 28 GHz and 38 GHz in an urban low-rise environment. The clutter loss was found to depend on the placements of the Tx and Rx antennas among buildings. In [5], clutter loss measurements were conducted at 27 GHz in urban campus environment. The maximum clutter loss was about 35 dB. In [6, 7], clutter loss measurements were conducted at 26 GHz and 40 GHz in suburban environments in the range of 120-350 m. The clutter loss with respect to the elevation angle range of 0°-5° was analyzed. In addition, ray tracing simulation results were compared with the measurement results. In [8], the clutter loss and building entry loss were measured at 26 GHz. Building entry loss was higher than clutter loss above the median value due to measurements taken on the higher floors. In [9], above rooftop channel measurements were conducted in a suburban environment at 32.4 GHz. The paths along the road, between houses, and on the roof were measured. A site-specific path loss and clutter loss model was proposed. In [10], an overview of the new developed ITU-R P.2108-0 model was given. Extensive measurements in Aalborg, Gothenburg, and Tokyo were presented. The clutter loss in Aalborg was measured in a residential area at 18 GHz band with distances up to 1.4 km. A clear increasing trend of clutter loss was found up to 0.8 km, while it became constant for larger distances. The clutter loss in Tokyo was measured at 2.2, 4.7, 26.4, and 66.5 GHz in the range of 0.26-1.2 km.

In this paper, we present clutter loss measurements at 26 GHz, as it is one of the “pioneer bands” in Europe and identified by ITU WRC-19 recently for fifth generation (5G) high data rate transmission. The results are compared with the ITU-R P.2108-0 statistical clutter loss model.

The remainder of the paper is organized as follows. Section 2 describes the 26 GHz clutter loss measurements. The ITU-R P.2108-0 statistical clutter loss model is presented in Section 3. The measurement and modeling results and analysis are given in Section 4. Finally, conclusions are drawn in Section 5.

2 26 GHz Clutter Loss Measurements

The custom-designed channel sounder [11] is used to conduct 26 GHz clutter loss measurements along three

routes at Durham University, behind buildings indicated as (R1), (R2), and (R3), shown in Fig. 2(a)-(c). The Tx is located at a height of about 18.2 m with a down tilt angle of 12°, as shown in Fig. 2(d). The measured frequency band is 24.68-27.68 GHz at a sweep repetition frequency of 1.22 kHz. A horn antenna with 20 dBi gain and 18° beamwidth is used at the Tx side, while an omni-directional antenna is used at the Rx side with a height of 1.6 m. The main beam of the Tx antenna is adapted to cover the three measurement routes, as shown in Fig. 2(e). A total of 102, 150, and 47 positions were measured in R1, R2, and R3, respectively. The corresponding Tx-Rx distances were 50-80 m, 60-100 m, and 100-105 m for the three routes, respectively.

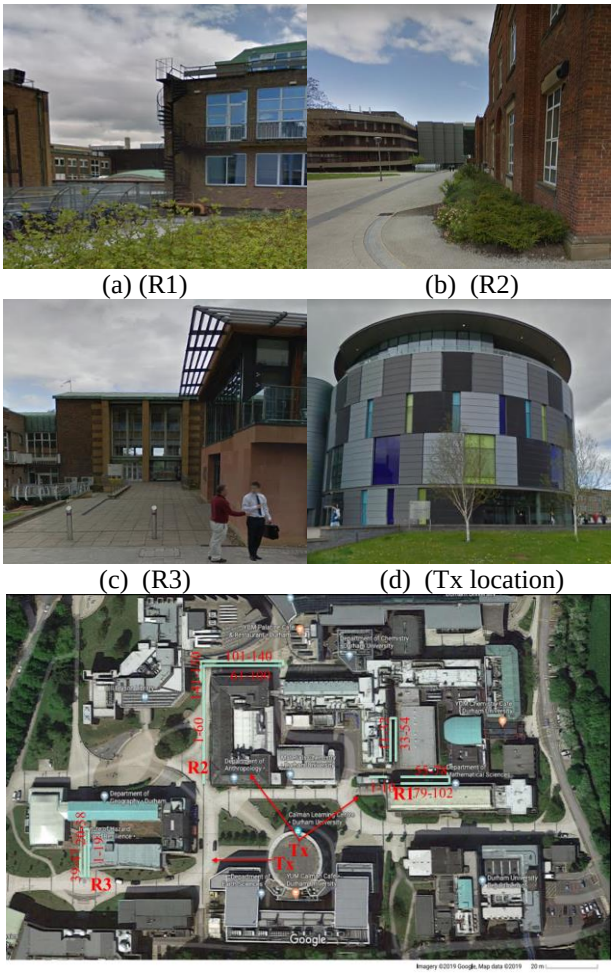

(a) (R1) (b) (R2)

(c) (R3) (d) (Tx location)

(e) Measurement setup

Figure 2. Clutter loss measurement environments.

3 Statistical Clutter Loss Model

In ITU-R P.2108-0 recommendation, there are three clutter loss models, for different terminal environments and frequency ranges. The statistical clutter loss model for the frequency range of 2-67 GHz is applied to model the 26 GHz clutter loss.

In the statistical clutter loss model, the input parameters include frequency f (GHz), Tx-Rx distance d (km), and percentage of locations p (%). The clutter loss not exceeded for p% of locations for the terrestrial to terrestrial path is given as

$$L_{ctt} = -5\log(10^{-0.2L_l} + 10^{-0.2L_s}) - 6Q^{-1}(p/100)\ \text{dB} \quad (1)$$

$$L_l = 23.5 + 9.6\log(f)\ \text{dB} \quad (2)$$

$$L_s = 32.98 + 23.9\log(d) + 3\log(f)\ \text{dB} \quad (3)$$

where Q^{-1}(p/100) is the inverse complementary normal distribution function, L_l and L_s are the long-range and short-range clutter loss, respectively [10]. An illustration of the median clutter loss calculated from the model is shown in Fig. 3. As the frequency increases, the median clutter loss becomes larger. Below the distance of about 1 km, the median clutter loss shows a linear relationship with the distance in log scale. When the distance becomes larger, the median loss does not change, i.e., goes to the saturation range.

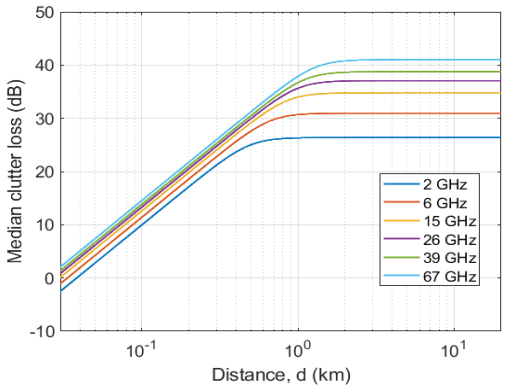

Figure 3. An illustration of the median clutter loss calculated from the ITU-R P.2108-0 clutter loss model.

4 Results and Analysis

The measured power delay profile (PDP) is expressed as

$$PDP = \sum_{l=1}^{L} p_l\, \delta(\tau - \tau_l) \quad (4)$$

where L is the number of multipath components (MPCs) with powers above the threshold, p_l and τ_l are the power and delay of the lth MPC, respectively.

The clutter loss can be calculated as

$$CL = P - FSPL \quad (5)$$

$$P = \sum_{l=1}^{L} p_l \quad (6)$$

$$FSPL = 20log_{10}(\frac{4\pi df}{c}) \quad (7)$$

where P and $FSPL$ are the total path loss and free space path loss, respectively.

The measured PDPs and path loss variations of R1, R2 and R3 are shown in Figs. 4-6, respectively. As can be seen, R1 shows a low probability of clutter loss, which is possible for a short link. R2 has the largest clutter loss as the buildings are high and dense, which causes higher losses. R3 has the smallest clutter loss variation, as the distance variations are over a small range. The measurement results show high correlation with the building geometry and surrounding environments.

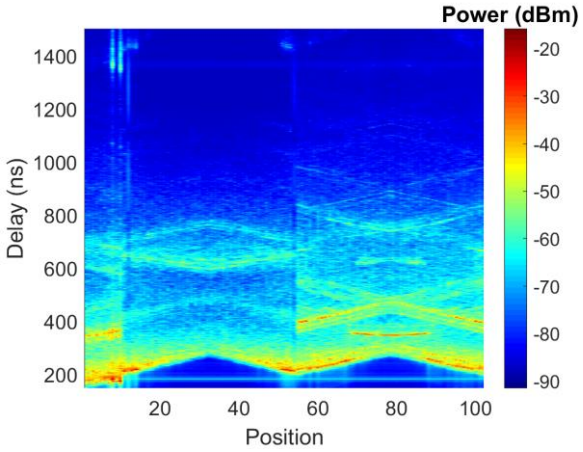

(a) Measured PDPs of R1.

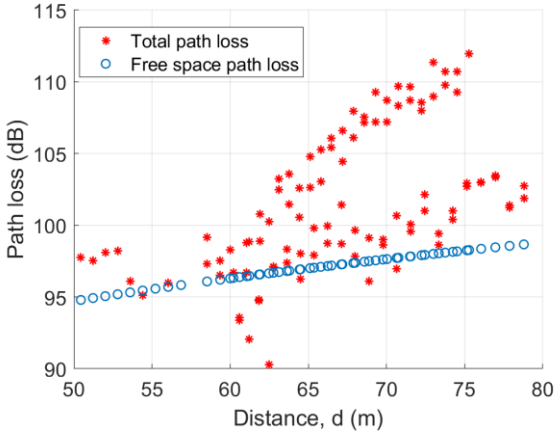

(b) Path loss variations of R1.

Figure 4. Measured PDPs and path loss variations of R1.

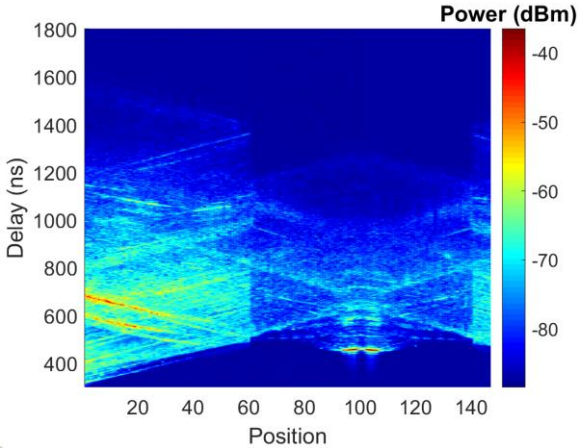

(a) Measured PDPs of R2.

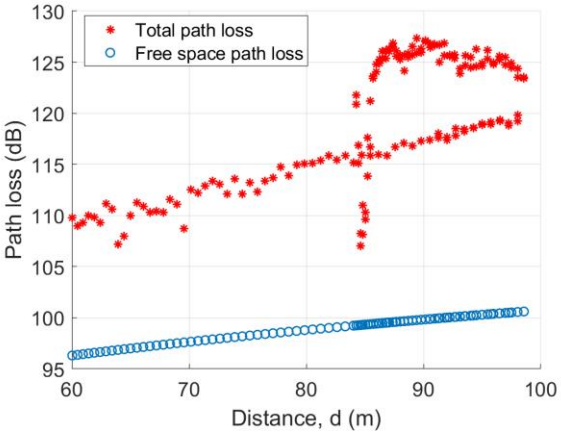

(b) Path loss variations of R2.

Figure 5. Measured PDPs and path loss variations of R2.

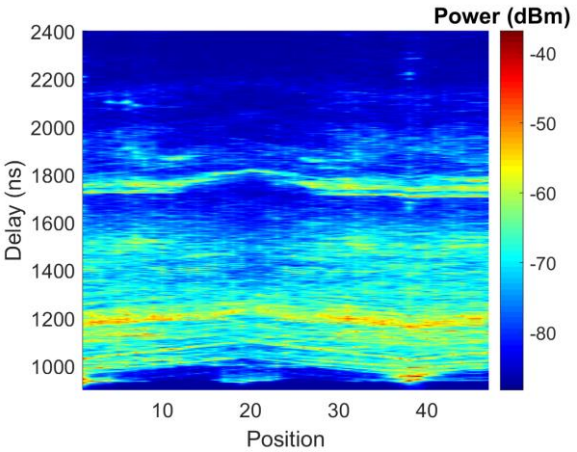

(a) Measured PDPs of R3.

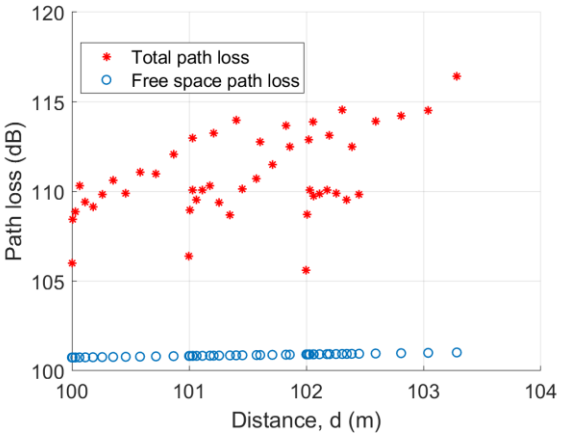

(b) Path loss variations of R3.

Figure 6. Measured PDPs and path loss variations of R3.

The measured cumulative distribution functions (CDFs) for R1, R2, and R3 are shown in Fig. 7. R1 has the smallest clutter loss, while R2 has the largest clutter loss. A comparison of the measured and modeled clutter losses is shown in Fig. 8. For the statistical clutter loss model, as the distance increases from 70 m to 90 m, the clutter loss tends to be larger. For the measurement results, the distance is in the range of 50-105 m. To avoid statistical

bias, the combined clutter loss values are re-sampled at some distances. The measured combined CDF is closest to the statistical clutter model when d = 80 m. The measured median clutter loss is 11 dB, which is similar to the statistical clutter model when d = 80 m. The comparison shows a good match between measured and modeled clutter loss.

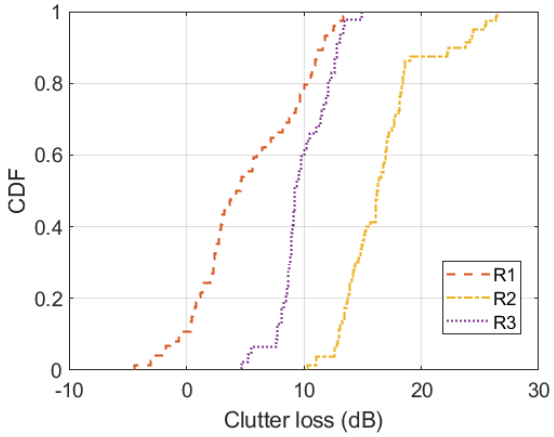

Figure 7. CDFs of the measured clutter loss.

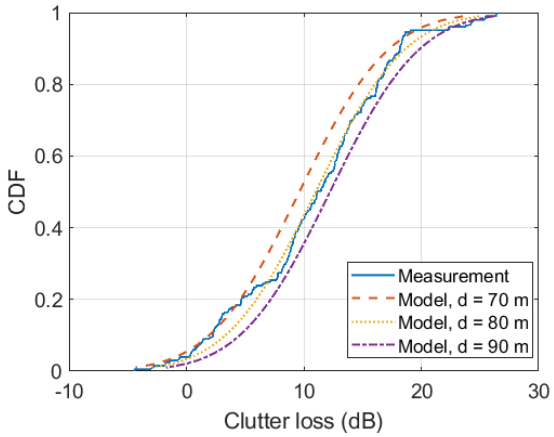

Figure 8. Comparison of the measured and modeled clutter losses.

5 Conclusions

In this paper, results of measurements conducted at 26 GHz using the customized channel sounder at Durham University were presented. The measurement data were processed to extract clutter loss. The ITU-R P.2108-0 statistical clutter loss model was utilized to model the clutter loss at 26 GHz band. The clutter loss is found to be related to the building geometry and surrounding environment and the measured and modeled clutter loss have shown good agreement.

6 Acknowledgements

The authors would like to acknowledge the support of WaveComBE project, under Horizon 2020 research and innovation program, grant agreement No. 766231, the European Joint Research Centre, JRC, Ispra, Italy, EPSRC under grant EP/I01049/1, PATRICIAN, and Intel, USA. The authors would also like to acknowledge Amar Al-Jzari and Mohamed Abdulali at Durham University for their help in conducting the channel measurements.

7 References

1. ITU-R P.2108-0, Prediction of clutter loss, June 2017.
2. C. Hammerschmidt, R. Johnk, "Extracting clutter metrics from mobile propagation measurements in the 1755–1780 MHz band," in *Proc. IEEE MILCOM'16*, Baltimore, MD, USA, Nov. 2016, pp. 1-6.
3. R. Rudd, D. Wu, V. Ocheri, M. Nekovee, "Independent and joint statistics of clutter loss and building entry loss—Initial measurements," in *Proc. IEEE PIMRC'18*, Bologna, Italy, Apr. 2018, pp. 1-2.
4. Y. Yoon, J. Kim, K. Kim, M. Kim, Y. Chong, "Clutter loss characteristic in mm-Wave bands for small urban environment," in *Proc. ICTC'17*, Jeju, South Korea, Oct. 2017, pp. 1-3.
5. R. F. Rudd, M. Nekovee, "Millimetre-wave propagation in urban clutter for 5G systems," in *Proc. LAPC'17*, Loughborough, UK, Nov. 2017, pp. 1-2.
6. B. Montenegro-Villacieros, J.-M. Chareau, J. Bishop, P. Viaud, T. Pinato, M. Basso, "Clutter loss measurements in suburban environment at 26 GHz and 40 GHz," in *Proc. EuCAP'18*, London, UK, Apr. 2018, pp. 1-4.
7. B. Montenegro-Villacieros, J. Bishop, J.-M. Chareau, "Clutter loss measurements and simulations at 26 GHz and 40 GHz," in *Proc. EuCAP'19*, Krakow, Poland, Mar.-Apr. 2019, pp. 1-5.
8. S. Salous, F. Tufvesson, K. Turbic, L. M. Correia, T. Kürner, D. Dupleich, C. Schneider, D. Czaniera, B. M. Villacieros, "IRACON propagation measurements and channel models for 5G and beyond," *ITU Journal: ICT Discoveries*, **2**, 1, Nov. 2019, pp. 1-9.
9. Y. K. Yoon, K. W. Kim, Y. J. Chong, "Site prediction model for the over rooftop path in a suburban environment at millimeter wave," *International Journal of Antennas and Propagation*, **2019**, Article ID 1371498, Apr. 2019, pp. 1-12, doi:10.1155/2019/1371498.
10. J. Medbo, C. Larsson, B.-E. Olsson, F. S. Chaves, H. C. Nguyen, I. Rodriguez, T. B. Sorensen, I. Z. Kovács, P. Mogensen, K.-T. Lee, J. Woo, M. Sasaki, W. Yamada, "The development of the ITU-R terrestrial clutter loss model," in *Proc. EuCAP'18*, London, UK, Apr. 2018, pp. 1-6.
11. S. Salous, S. M. Feeney, X. Raimundo, and A. A. Cheema, "Wideband MIMO channel sounder for radio measurements in the 60 GHz band," *IEEE Trans. Wireless Commun.*, **15**, 4, pp. 2825-2832, Apr. 2016.